

Itinerant Antiferromagnetism in Infinite Dimensional Kondo Lattice

Shintaro Hoshino, Junya Otsuki, and Yoshio Kuramoto
Department of Physics, Tohoku University, Sendai 980-8578
(Dated: November 27, 2018)

Highly accurate numerical results for single-particle spectrum and order parameter are obtained for the magnetically ordered Kondo lattice by means of the dynamical mean-field theory combined with the continuous-time quantum Monte Carlo method. Hybridized energy bands involving local spins are identified in the Néel state as a hallmark of itinerant antiferromagnetism. At the boundary of the reduced Brillouin zone, the two-fold degeneracy remains in spite of the doubled unit cell. This degeneracy results if the molecular field felt by localized spins has identical magnitude and reversed direction with that of conduction electrons. The persistent Kondo effect is responsible for the behavior. The antiferromagnetic quantum transition occurs inside the itinerant regime, and does not accompany the itinerant-localized transition.

Distinction between itinerant and localized characters of strongly correlated electrons has been one of the most fundamental issues in condensed-matter physics. The Kondo effect plays a central role in this problem because even a localized spin may acquire itinerant character by coupling with conduction electrons, and may form a Fermi liquid. Some of recent experiment suggest that quantum phase transition between magnetic and paramagnetic ground states accompanies a change between localized and itinerant character of electrons, with non-Fermi liquid behavior in the vicinity of the transition [1]. Another experiment using the de Haas-van Alphen effect has probed the change of the Fermi surface as the external pressure drives such systems as CeIn₃ and CeRhIn₅ across the magnetic transition [2]. On the other hand, recent photoemission experiment for CeRu₂Si₂ and CeRu₂Si_{2-x}Ge_x indicates that the Fermi surfaces of both are essentially the same, which involve f electrons and are referred to as the large Fermi surface. The experiment is performed at temperatures above the Néel transition of CeRu₂Si_{2-x}Ge_x [3], while CeRu₂Si₂ remains paramagnetic down at least to 0.1 K. Thus the antiferromagnetism in CeRu₂Si_{2-x}Ge_x seems to be itinerant. Consistent understanding of this variety of phenomena is still lacking, and accurate theoretical analysis is necessary to understand how the magnetic order is related to the change from itinerant to localized characters of electrons.

In this paper we show that the antiferromagnetism in the Kondo lattice model (KLM) occurs within the itinerant regime. The KLM is the simplest system that is capable of describing both itinerant and localized characters of electrons, and is given by

$$\mathcal{H} = \sum_{\mathbf{k}\sigma} \varepsilon_{\mathbf{k}} c_{\mathbf{k}\sigma}^\dagger c_{\mathbf{k}\sigma} + 2J \sum_i \mathbf{S}_i \cdot \mathbf{s}_{ci}, \quad (1)$$

where the first term represents the kinetic energy of conduction electrons, \mathbf{S}_i is the localized spin at site i , and \mathbf{s}_{ci} denotes the conduction-electron spin at the same site. In terms of creation $c_{i\alpha}^\dagger$ and annihilation $c_{i\alpha}$ operators of conduction electrons at site i with spin α , we obtain

$\mathbf{s}_{ci} = \frac{1}{2} \sum_{\alpha\beta} c_{i\alpha}^\dagger \boldsymbol{\sigma}_{\alpha\beta} c_{i\beta}$. The KLM has been investigated beyond the mean field theory in one- [4, 5] and two- [6, 7, 8, 9, 10] dimensional systems. We approach the KLM from infinite dimensions using the dynamical mean-field theory (DMFT) to allow for the Néel state at finite temperatures. We use the continuous-time quantum Monte Carlo method (CT-QMC) [11, 12, 13] as the impurity solver, and focus on the case of unit number $n_c = 1$ of conduction electrons per site. In contrast with the metallic antiferromagnetism with $n_c \neq 1$, where an incommensurate order may exist, we can safely assume the simple staggered order because of the nesting condition for the conduction band in the hypercubic lattice. Hence the results in this paper are exact in infinite dimensions except for statistical errors.

As the half-filled limit is approached from $n_c \neq 1$, the large Fermi surface tends to the zone boundary of the paramagnetic phase, while the small Fermi surface involves half of the Brillouin zone volume. Provided that the ground state has no discontinuity in the zero-doping limit, the limiting location of the Fermi surface should be reflected in the location of the energy gap in the half-filled case. In the localized antiferromagnetism, the gap opens at the boundary of the new Brillouin zone since conduction electrons feel the staggered internal field. In itinerant magnetism, on the other hand, we show in this paper that the energy gap is located in the center of the new Brillouin zone. The zone-center location is due to emergence of energy bands of magnetic electrons. Hence location of the energy gap distinguishes between itinerant and localized behaviors. Note that such distinction does not apply to the single band model such as the Hubbard model where the energy gap in the half-filled limit always occurs in the boundary of the Brillouin zone. In this case the character of electrons changes continuously from the itinerant limit to the localized one as the Coulomb repulsion increases relative to the band width.

We take the bare density of states

$$\rho_c(\omega) = \sqrt{2/\pi} \exp(-2\omega^2) \quad (2)$$

which corresponds to infinite-dimensional hypercubic lat-

tice. We have taken the band width $D = 1$ as the unit of energy. For the Gaussian density of states, the Kondo temperature T_K is defined by

$$\rho_c(0)T_K = \frac{e^{-\gamma/2}}{\sqrt{\pi}} \exp\left(-\frac{1}{2\rho_c(0)J}\right), \quad (3)$$

where $e^{-\gamma/2}/\sqrt{\pi} \sim 0.42$ with $\gamma \simeq 0.577$ being the Euler constant. This expression of T_K corresponds to divergence of effective exchange in the lowest-order scaling equation.

The hypercubic lattice has the nesting property with the wave vector $\mathbf{Q} = (\pi, \pi, \dots)$ at half filling, which favors the staggered order. In the two-sublattice formalism, the Green function $\mathbf{G}_{\mathbf{k}\sigma}(z)$ of conduction electrons is a 2×2 matrix where z is a complex energy, and a wave vector \mathbf{k} belongs to the reduced Brillouin zone [14]. In the DMFT, the wave vector enters only through $\varepsilon_{\mathbf{k}}$. Therefore we introduce the notation $\kappa = \varepsilon_{\mathbf{k}}$, and regard κ as if it represents a wave number. The spectral function $A_\sigma(\kappa, \omega)$ can be calculated from the matrix Green function $\mathbf{G}_\sigma(\kappa, z)$ as

$$A_\sigma(\kappa, \omega) = -\text{Im} [\text{Tr} \mathbf{G}_\sigma(\kappa, \omega + i\delta)] / \pi. \quad (4)$$

Then the renormalized density of states $\rho_\sigma(\omega)$ is given by $\rho_\sigma(\omega) = 2N^{-1} \sum_{\mathbf{k}} A_\sigma(\varepsilon_{\mathbf{k}}, \omega)$ where the summation runs over the reduced Brillouin zone with $N/2$ points. In the paramagnetic state, the reduced number of \mathbf{k} is compensated by the trace over $\mathbf{G}_{\mathbf{k}\sigma}(z)$ to give the same $\rho_\sigma(\omega)$ as derived by use of the original Brillouin zone. Even in the Néel state, $\rho_\sigma(\omega)$ does not depend on σ because of summation over sublattices.

Let us first discuss the magnitude of the staggered moment given by $2\langle S_Q^z \rangle = \langle S_A^z \rangle - \langle S_B^z \rangle$, where we choose the positive polarization for the A sublattice. Figure 1 shows the temperature dependence of the staggered moment, which should vanish at the Néel temperature T_N . On the other hand, the staggered magnetic susceptibility χ_Q in the paramagnetic state should diverge as the temperature is lowered toward T_N . Hence we also plot χ_Q^{-1} calculated in ref.[15]. It is found that the estimates of T_N by $\langle S_Q^z \rangle$ and by χ_Q^{-1} are consistent with each other. However, calculation of $\langle S_Q^z \rangle$ becomes increasingly difficult as T is approached to T_N . The results shown in FIG.1 are restricted to the temperature range where we could obtain reliable values. With $J = 0.1$, the localized spins are almost fully polarized in the ground state. As J increases, $\langle S_Q^z \rangle$ decreases by the Kondo effect, which eventually suppresses the antiferromagnetism at $J = J_c \simeq 0.27$ down to $T = 0$.

We next discuss the density of states near $T = 0$, which is derived using the Padé approximation for analytic continuation from imaginary Matsubara frequencies $i\varepsilon_n$ to the real ones. Since the Monte Carlo data are obtained accurately in the imaginary time domain, the Padé approximation works well in the CT-QMC method[13].

Figure 2 shows $\rho_\sigma(\omega)$ for different values of J near the ground state. Namely, we take the temperature where the density of states does not vary much when T decreases further. For example, we take $T = 0.01$ for $J = 0.3$, but $T = 0.002$ for $J = 0.1$. The present method has no difficulty to go to such low temperatures with high accuracy. In the case of $J = 0.3$ with the paramagnetic ground state, the density of states has a gap caused by the Kondo effect. The state is often called the Kondo insulator. In the case of $J = 0.26$, the ground state is antiferromagnetic as seen from FIG.1. The density of states in the ordered phase is almost the same as that with $J = 0.3$. Namely the density of states does not depend much on whether the ground state is paramagnetic or antiferromagnetic as far as J is close to the critical value J_c .

When J is smaller, sharp peaks develop at both edges of the gap. The origin is understood as follows: Putting the self-energy of conduction electrons as the staggered potential $\pm h$ by the Néel order, we obtain

$$\text{Tr} \mathbf{G}_\sigma(\kappa, z) = \frac{1}{z + \sqrt{\kappa^2 + h^2}} + \frac{1}{z - \sqrt{\kappa^2 + h^2}}. \quad (5)$$

Then the density of states is given by

$$\rho_\sigma(\omega) = \frac{2|\omega|}{\sqrt{\omega^2 - h^2}} \rho_c(\sqrt{\omega^2 - h^2}), \quad (6)$$

with a square-root divergence at both edges $\omega = \pm h$. For $\omega^2 < h^2$, we obtain $\rho_\sigma(\omega) = 0$. This form of $\rho_\sigma(\omega)$ roughly explains the peak structure with $J = 0.1$ in FIG.2. In the numerical result, the residual Kondo effect actually suppresses the divergence in $\rho_\sigma(\omega)$.

On the other hand, the density of states for larger J does not show a clear threshold. The Gaussian tail in the bare density of states $\rho_c(\omega)$ causes a tiny but finite magnitude of $\rho_\sigma(\omega)$ within the apparent energy gap. Therefore

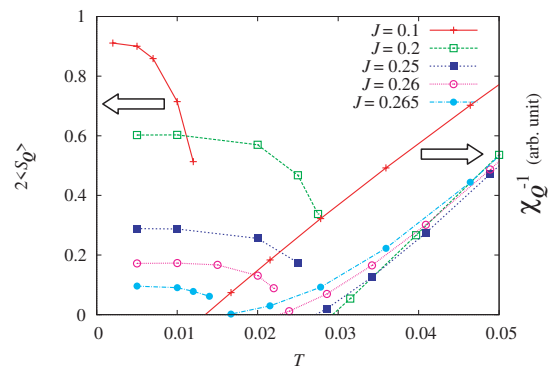


FIG. 1: (color online) Staggered spin polarization $2\langle S_Q^z \rangle$ (left scale) as a function of temperature for different values of J . Also shown is the inverse staggered susceptibility χ_Q^{-1} (right scale), which goes to zero at T_N

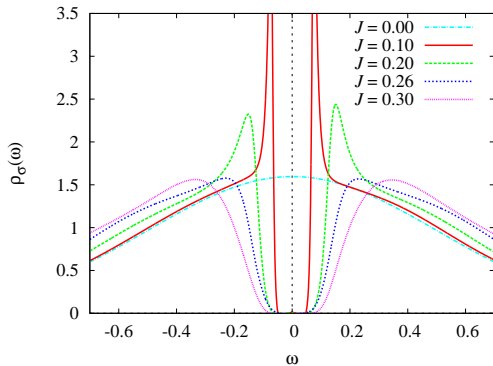


FIG. 2: (color online) J dependence of the density of states for the conduction electron and with $T \sim 0$.

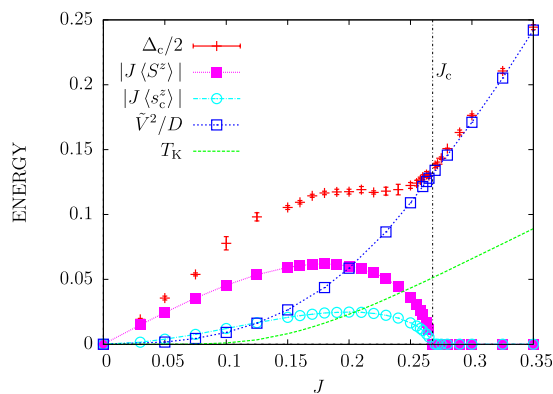


FIG. 3: (color online) J dependence of the energy gap $\Delta_c/2$. For comparison, also plotted are $J\langle S^z \rangle$, $J\langle s_c^z \rangle$, S^z and s_c^z are the localized and conduction spins at a local site, respectively. \tilde{V}^2/D represents the effective hybridization to be explained later, and T_K is the Kondo temperature defined by Eq.(3).

we introduce the characteristic value Δ_c of the energy gap as giving the half-maximum value of the peak in the density of states. Figure 3 shows $\Delta_c/2$ as a function of J . The error bars have been estimated from 5 bins of data. It is clear that Δ_c changes continuously at $J = J_c$. This shows that both Kondo effect and the staggered internal field are contributing to Δ_c . For $J \lesssim 0.1$, on the other hand, $\Delta_c/2$ is almost proportional to J . This behavior shows that the gap is mainly determined by the staggered field $J\langle S^z \rangle$ as shown also in FIG. 3.

The details of the itinerancy are seen in the single-particle spectral function $A_\sigma(\kappa, \omega)$. Figure 4 shows the spectrum in the case $J = 0.2$ where the Kondo effect is significant. In both paramagnetic and ordered phases, the spectrum consists of four bands in the reduced Brillouin zone. In the paramagnetic phase shown in the left panel, the new bands are ascribed to “hybridization bands” caused by the Kondo effect [16]. We note that there is no real hybridization between the f -electron and

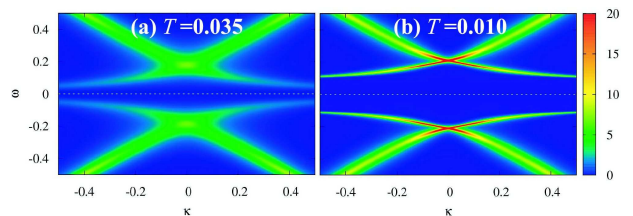


FIG. 4: (color online) Single-particle spectrum with $J = 0.2$ in (a) paramagnetic phase at $T = 0.035$ and (b) antiferromagnetic phase at $T = 0.010$.

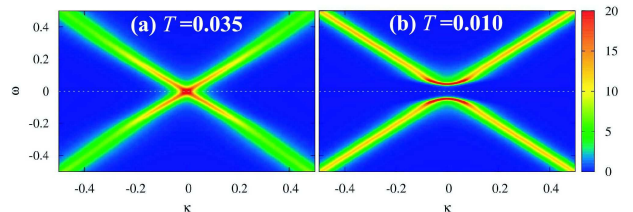


FIG. 5: (color online) $A_\sigma(\kappa, \omega)$ with ferromagnetic interaction $J = -0.2$ in (a) paramagnetic phase at $T = 0.035$ and (b) antiferromagnetic phase at $T = 0.010$.

the conduction electron because the f -electron does not have the charge degrees of freedom in the KLM. In the Brillouin zone of the paramagnetic state, the energy gap is indirect from the zone boundary to the zone center, both of which correspond to $\kappa \rightarrow \pm\infty$ in FIG.4. In the right panel of FIG.4(b), these hybridization bands are clearly seen even in the antiferromagnetic phase. Hence we classify the antiferromagnetism in this regime as itinerant.

Let us now present the spectrum in the ferromagnetic KLM for comparison, where each site forms $S = 1$ state with antiferromagnetic intersite interaction. The Kondo effect is absent in the case of $J < 0$. We can apply the CT-QMC method also to ferromagnetic J as noted in ref. [17]. Figure 5 shows the spectrum with the same T as in FIG.4. In the paramagnetic state shown in FIG.5(a), the spectrum is almost the same as the original conduction band. On the other hand, in the antiferromagnetic phase shown in FIG.5(b), the spectrum shows the clear gap structure. These behaviors are explained well by Eq.(5) with $h = 0$ in FIG.5(a), while $h \neq 0$ in (b). In the case of ferromagnetic J , the number of bands is two in contrast to the case with $J > 0$ with four bands.

Thus, the itinerant or localized behavior can be distinguished by the number of energy bands in the reduced Brillouin zone. Moreover the location of the energy gap is at the zone boundary in the localized case, but at the zone center in the itinerant case. Note that $\kappa = \pm\infty$ correspond to the lower and upper edges of the conduction band in infinite dimensions. Both edges come to the

center in the reduced Brillouin zone.

We note another characteristic feature in FIG.4(b) that the degeneracy at $\kappa = 0$ remains in the antiferromagnetic phase. A toy model helps to understand the origin of the degeneracy. Let us consider a non-interacting periodic Anderson model under staggered field as

$$\begin{aligned} \mathcal{H}_{\text{PAM}} = & \sum_{\mathbf{k}\sigma} \varepsilon_{\mathbf{k}} c_{\mathbf{k}\sigma}^\dagger c_{\mathbf{k}\sigma} + V \sum_{i\sigma} (f_{i\sigma}^\dagger c_{i\sigma} + \text{h.c.}) \\ & + 2 \sum_i (h_i s_{ci}^z + H_i S_i^z), \end{aligned} \quad (7)$$

where $f_{i\sigma} (f_{i\sigma}^\dagger)$ is the annihilation (creation) operator of an f -electron at the i site with the hybridization V . The staggered fields represent the molecular field associated with the antiferromagnetism. Then we choose $h_i = \pm h$ and $H_i = \pm H$, where the A (B) sublattice has the positive (negative) sign.

There are four branches associated with c and f degrees of freedom for the electrons, as well as presence of A and B sublattices. At $\kappa = 0$, we obtain the energies

$$E(\kappa = 0) = \pm \frac{1}{2} \left[(h + H) \pm \sqrt{(h - H)^2 + 4V^2} \right]. \quad (8)$$

If the relation $h = -H$ holds, $E(\kappa = 0)$ has only two distinct values both of which are doubly degenerate. We interpret the degeneracy in FIG.4(b) as caused by the relation $h = -H$ for the molecular field. We call such situation ‘‘quasi-local compensation’’. Note that the magnitudes of the polarization for the conduction spin $J\langle s_c^z \rangle$ and localized spin $J\langle S^z \rangle$ are much different as shown in FIG.3. Hence the actual energy level is determined not by the local internal field, but by a long-range field involving remote conduction electrons. The compensation is reminiscent of the spatially extended Kondo singlet with small J .

Let us identify the energy scale in the Néel state from the self energy. For sublattice $\alpha = \pm 1$ and spin $\sigma = \pm 1$, $\Sigma_{\alpha\sigma}(z)$ is expanded as

$$\Sigma_{\alpha\sigma}(z) = \alpha\sigma h + \frac{\tilde{V}^2}{z} + O\left(\frac{1}{z^2}\right), \quad (9)$$

where \tilde{V} is the effective hybridization. The coefficient \tilde{V}^2 of $1/z$ corresponds to the jump at $\tau = 0$ in the imaginary time domain. We extract numerically the coefficient \tilde{V}^2 of $1/i\varepsilon_n$ in the self energy. Figure 3 shows the result for \tilde{V}^2/D ($= \tilde{V}^2$) as a function of J . Note that the indirect energy gap in the toy model (7) is given by V^2/D . The agreement between \tilde{V}^2/D and $\Delta_c/2$ in the paramagnetic phase is excellent. However, this consistency should not be taken too seriously because Δ_c depends on the definition of the gap. We emphasize that \tilde{V}^2/D shows no anomaly across the phase transition to the antiferromagnetic phase. It also shows good proportionality to the Kondo temperature as $\tilde{V}^2/D \simeq 2.6T_K$.

In the region $0 < J \lesssim 0.1$, the Néel temperature T_N is much larger than T_K as seen from FIGS.1 and 3. The electronic state at the transition has a localized character since the Kondo effect is negligible at T_N . Namely there is no hybridized band, and the energy gap occurs at the boundary of the reduced Brillouin zone. However, we have checked that two almost flat bands appear newly below T_K even with $J = 0.05$. Hence, the crossover from localized behavior to the itinerant one occurs inside the Néel ordered state.

In summary, we have derived single-particle spectrum and the temperature-dependent order parameter in the infinite dimensional KLM allowing for the Néel order. The high numerical accuracy has made it possible to find the quasi-local compensation between the conduction and localized spins indicating the persistent tendency toward the Kondo singlet at each site. The effective hybridization energy has no anomaly across the quantum phase transition, and scales well with the impurity Kondo temperature T_K . Hence the quantum transition into antiferromagnetism occurs within the itinerant regime, and does not involve itinerant-localized transition.

-
- [1] P. Gegenwart, Q. Si, and F. Steglich: Nature Phys. **4** (2008) 186.
 - [2] R. Settai, T. Takeuchi, and Y. Onuki: J. Phys. Soc. Jpn. **76** (2007) 051003.
 - [3] T. Okane *et al*: Phys. Rev. Lett. **102** (2009) 216401.
 - [4] H. Tsunetsugu, M. Sigrist and K. Ueda: Rev. Mod. Phys. **69** (1997) 809.
 - [5] N. Shibata and H. Tsunetsugu: J. Phys. Soc. Jpn. **68** (1999) 744;
 - [6] F. F. Assaad: Phys. Rev. Lett. **83** (1999) 796.
 - [7] S. Capponi and F. F. Assaad: Phys. Rev. B **63** (2001) 155114.
 - [8] H. Watanabe and M. Ogata: Phys. Rev. Lett **99** (2007) 136401.
 - [9] L. C. Martin and F. F. Assaad: Phys. Rev. Lett **101** (2008) 066404.
 - [10] N. Lanatà, P. Barone, and M. Fabrizio: Phys Rev B **78** (2008) 155127.
 - [11] A. N. Rubtsov, V. V. Savkin, and A. I. Lichtenstein: Phys. Rev. B **72** (2005) 035122.
 - [12] P. Werner and A. J. Millis: Phys. Rev. B **74** (2006) 155107.
 - [13] J. Otsuki, H. Kusunose, P. Werner, and Y. Kuramoto: J. Phys. Soc. Jpn. **76** (2007) 114707.
 - [14] A. Georges, G. Kotliar, W. Krauth, and M. J. Rozenberg: Rev. Mod. Phys. **68** (1996) 13.
 - [15] J. Otsuki, H. Kusunose, and Y. Kuramoto: J. Phys. Soc. Jpn. **78** (2009) 034719 .
 - [16] J. Otsuki, H. Kusunose, and Y. Kuramoto: Phys. Rev. Lett. **102** (2009) 017202.
 - [17] S. Hoshino, J. Otsuki, and Y. Kuramoto: J. Phys. Soc. Jpn. **78** (2009) 074719.